

## Mechanism of scaling on oxidation reactor wall in TiO<sub>2</sub> synthesis by chloride process

ZHOU E(周 峨)<sup>1</sup>, YUAN Zhang-fu(袁章福)<sup>1</sup>, WANG Zhi(王 志)<sup>1</sup>,  
FANG Xian-Guo(范先国)<sup>2</sup>, GONG Jia-Zhu(龚家竹)<sup>2</sup>

1. Institute of Process Engineering, Chinese Academy of Sciences, Beijing 100080, China;

2. Sichuan Lomon Corporation, Mianzhu 618200, China

Received 20 June 2005; accepted 25 November 2005

**Abstract:** The mechanism of scaling on the oxidation reactor wall in TiO<sub>2</sub> synthesis process was investigated. The formation of wall scale is mostly due to being deposited and sintered of TiO<sub>2</sub> particle formed in the gas phase reaction of TiCl<sub>4</sub> with O<sub>2</sub>. The gas-phase oxidation of TiCl<sub>4</sub> was in a high temperature tubular flow reactor with quartz and ceramic rods put in center respectively. Scale layers are formed on reactor wall and two rods. Morphology and phase composition of them were characterized by transmission electron microscope(TEM), scan electron micrographs(SEM) and X-ray diffraction(XRD). The state of reactor wall has a little effect on scaling formation. With uneven temperature distribution along axial of reactor, the higher the reaction temperature is, the thicker the scale layer and the more compact the scale structure is.

**Key words:** TiO<sub>2</sub> synthesis; scaling; reactor wall; oxidation; chloride process

### 1 Introduction

Titania particles are synthesized by the gas-phase oxidation of titanium tetrachloride in a high temperature tubular flow reactor on a large industrial scale. This so-called chloride process has been reported by several researchers[1–5]. In contrast to the sulfate process, this chloride method is more cost effective and cleaner. But in the industrial operation, a serious problem is that a hard TiO<sub>2</sub> coating forms on the inner surface of oxidation reactor. The deposition of TiO<sub>2</sub> on the hot reactor wall will cause the generation of hard scale layer and alteration of the reactor efficient dimension and heat exchange efficiency. The worst of it is that the tube is blocked and the production must be shut down.

Some reasons of scale formation have not been uniform and they are explained as below. Tammann temperature of one kind of material is about half of its melting point temperature (referring to absolute temperature). When the heating temperature reaches Tammann temperature, most of solid material will be softened and viscous which easily cause sintering or scaling. The temperature of titania synthesis by chloride process is much higher than TiO<sub>2</sub> tammann temperature,

thus the initial formative TiO<sub>2</sub> particles are very easy to conglomerate on the reactor wall. According to heterogeneous nucleation law, the irregular reactor inside surface will be the nucleating points of gas-solid reaction[6,7]. Coagulation and agglomeration of ultrafine particles result in adherence and sedimentation of the formative powders and clusters to the reactor inner surface[8]. Although some techniques have been adopted to remove the scales, such as mechanical scraping, sand blasting and gas-film surrounding, the fundamentals of the process are not well understood and mechanism of the scale formation has not been further investigated.

In this paper, TiCl<sub>4</sub> was oxidized in the quartz tube flow reactor at a high temperature. As a contrast test of simulated reactor wall surface state, a glossy quartz rod and a rough ceramic rod were put in the reactor center respectively in order to study the scale distribution on the rods surface. Scale layers were formed on reactor wall and two rods. Morphology and phase composition of them were characterized by transmission electron microscope(TEM), scan electron micrographs(SEM) and X-ray diffraction(XRD). The effects of reactor wall surface state, radial growth of scale layer and reactor axial temperature distribution on scaling formation were discussed. At the same time, mechanism of scaling on the

reactor wall was explored further.

## 2 Experimental

The used raw materials were  $\text{TiCl}_4$  (99.5% pure), oxygen (99.99% pure), NaOH (chemically pure) and Ar (99.99% pure). A schematic diagram of the experimental apparatus is shown in Fig.1.

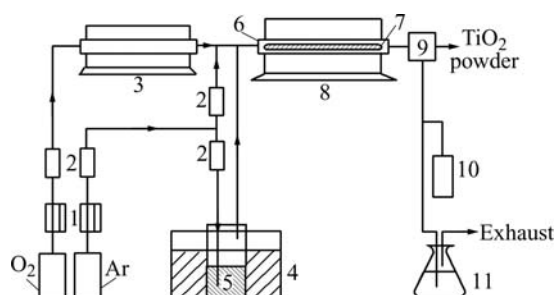


**Fig.1** Schematic of experimental apparatus: 1 Flow controller; 2 Rotameter; 3  $\text{O}_2$  preheater; 4  $\text{TiCl}_4$  preheater; 5  $\text{TiCl}_4$ ; 6 Quartz reactor; 7 Quartz rod; 8 Furnace; 9 Water cooler and separator; 10 Gas sampling; 11 Chlorine absorber

The reaction apparatus consisted of gas purifiers, reactant preheaters, reactor, water cooler and separator and an off-gas treatment unit. The reactor was a 27 mm in inner diameter (32 mm in out diameter), 1 430 mm in length quartz tube (99.8%  $\text{SiO}_2$ ), which was heated by a horizontal electrical furnace (Tianjin Zhonghuan Furnace Ltd Co). A quartz rod (99.8%  $\text{SiO}_2$ ) and a ceramic rod (95.5%  $\text{Al}_2\text{O}_3$ ), 6 mm in diameter, 1 000 mm in length were arranged in the reactor center respectively. Prepurified dry argon gas was used as a carrier gas and bubbled into a flask containing liquid  $\text{TiCl}_4$  in water bath (maintained at about  $90 \pm 1$  °C). This mixture of Ar and  $\text{TiCl}_4$  vapor was combined with another Ar stream for dilution and preheated  $\text{O}_2$  stream (at about 300 °C) and then flowed into the reactor tube. The flow of oxygen gas was usually in excess of the stoichiometric amount. The gas flow rate was ranged from 1.5 L/min to 3.5 L/min. Exiting from the furnace and reactor tube, the gas stream was cooled with room temperature dry  $\text{N}_2$  (99.95% pure) gas in a quartz jacketed cooler at the rear of the reactor. The cooling gas quenched chemical reaction and inhibited particle growth by coagulation at the outside of the reaction zone. The exhaust gas was neutralized with a 1 mol/L NaOH solution before exiting through the laboratory hood. All of the gas flows were monitored by rotameters. Lines transporting  $\text{TiCl}_4$  were maintained at 150 °C to prevent condensation of  $\text{TiCl}_4$  in the lines. The typical temperature for reaction operation was set at 1 100 °C.

Transmission electron microscope (TEM, Hitachi H-800) and scanning electron microscope (SEM, JEOL JSM-6700F) were used to observe the morphology of the

scales and  $\text{TiO}_2$  powders. Scanning electron microscope (SEM) images of the scales were obtained on a JEOL JSM-35CF microscope operating at 10 kV. The X-ray diffraction (XRD) was used to determine the phase composition of the scales. Samples of the scale powders and block (crushed into powder shape) for XRD analysis were collected from the reactor inside wall and rods surface, and the diffraction lines were recorded on a diffractometer (X'Pert PRO MPD, PANalytical, using  $\text{CuK}\alpha$ , 40 kV, 30 mA). The mass fraction of the anatase and rutile phases in the samples were calculated from the relative intensities of the strongest peaks corresponding to anatase and rutile as described by SPURR and MYERS[9].

## 3 Results and discussion

### 3.1 Reactor wall surface state

After generated by the deposition and sinter of  $\text{TiO}_2$  particles on the reactor wall, which was affected by surface state of wall, such as smoothness or ruggedness, would be formed on its surface.

At the end of oxidation reaction lasting for 50 min, the ceramic rod was covered with a hard scale layer composed by whisker and bud. At the site 200 mm away from gas entrance, the scale whisker was longest, which indicated that the oxidation reaction was the severest there. On the one hand, in this region, supersaturation degree of gas phase  $\text{TiO}_2$  was the greatest, so, high concentrated minimal particles were produced in homogeneous nucleation. On the other hand, the rough surface of ceramic rod was liable to be the nucleation centers in heterogeneous nucleation. The SEM images shown in Fig.2 are scale layers (by grinding treatment) and titania powders collected from ceramic rod. In these pictures, it is obviously that the size of scale is much larger than that of particle diameter.

The TEM images shown in Fig.3 are scale layers (by grinding treatment) and titania powders collected from quartz rod. Under the same reaction conditions, such as reacting temperature, reactants concentration and residence time, particles will still be sintered on the glossy surface of quartz rod and have the same morphology as that on the rough ceramic rod surface.

As a result, scale layer is always formed on the smooth surface of reactor wall as well as irregular. The irregular microstructure of the reactor inside which is easy to be the heterogeneous nucleation points will be blanketed as soon as the surface is coated with a  $\text{TiO}_2$  scale film. It can be deduced that once scales are formed, the effect of surface geometrical shape will be more important than its microstructure.

### 3.2 Radial growth of scale layer

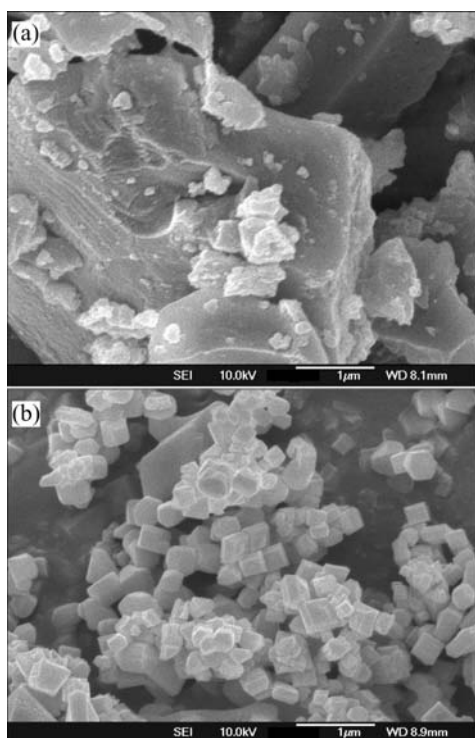


**Fig.2** SEM images of samples: (a) Wall scales of  $\text{TiO}_2$ ; (b)  $\text{TiO}_2$  powder

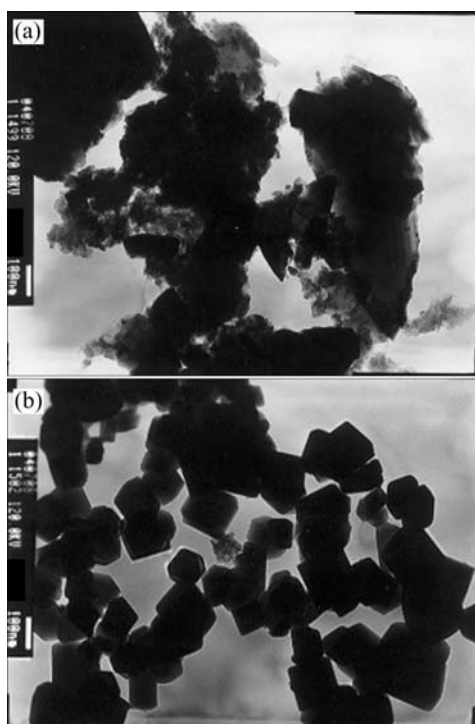


**Fig.3** TEM images of samples: (a) Wall scales of  $\text{TiO}_2$ ; (b)  $\text{TiO}_2$  powder

After gas-phase oxidation reaction finished, the reactor wall surface was coated with a thick rough scale layer. The thickness of scale layer along axial direction was varied. The scale layer at front reactor was much thicker than that at rear.

The SEM images shown in Fig.4 are the scale layer stripped from the reactor wall surface. Fig.4(a) shows a cross sectional profile of scale layer collected from major scaling zone. Seen from right side of scale layer, particles-packed is loose and this side is attached to the wall surface. Its positive face is shown in Fig.4(b). Seen from left side of scale layer, compact particles-sintered is tight and this side is faced to the reacting gases. Its local amplified top face is shown in Fig.4(c). Fig.5(a) shows the XRD patterns of the two sides of scale layer. Almost entire particles on sintered layer were characterized to be rutile phase. While, the particles on packed layer are anatase phase.

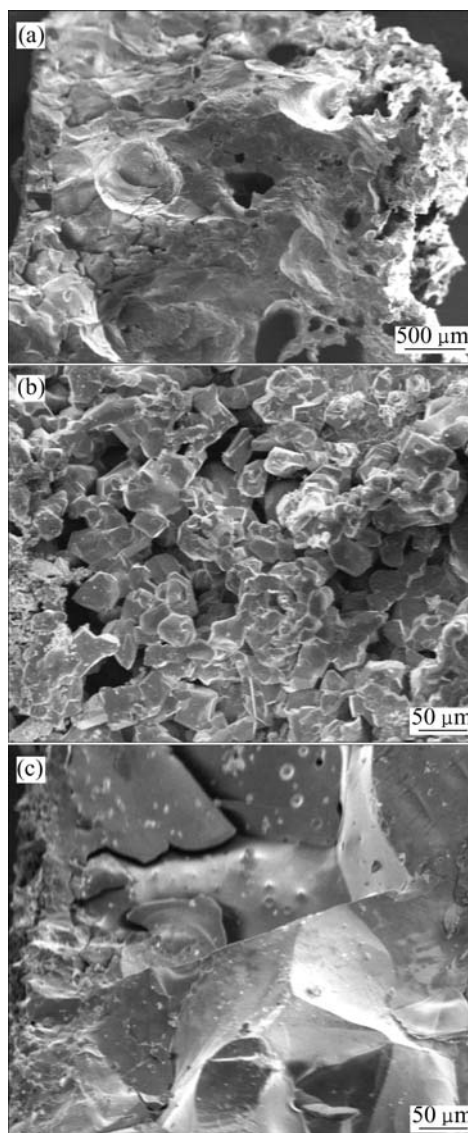


**Fig.4** SEM images of scale layers: (a) Scale layer profile; (b) Particles packed layer; (c) Sintering layer

As  $\text{TiO}_2$  particles are deposited on the reactor wall surface and the scale layer is formed, assuming that the cylindrical surface is considered flat surface and the heat accumulation generated by the thickness increase of

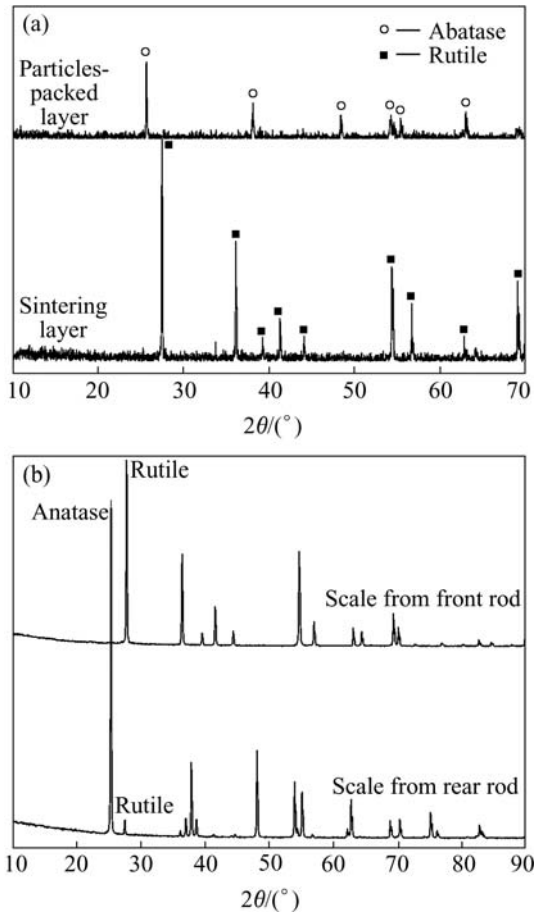


**Fig.5** XRD patterns of scale layers: (a) Scales from reactor wall surface; (b) Scales from rod

scale layer is neglected, the rate of heat transfer from reacting gases to the reactor wall surface can be expressed by

$$q = \frac{T_s - T_w}{\frac{\delta}{\lambda}} = \frac{T_g - T_s}{\frac{1}{\alpha}} \quad (1)$$

where  $T_s$  is the exterior surface temperature of scale layer,  $T_g$  is the reacting gases temperature,  $T_w$  is the reactor wall surface temperature,  $\delta$  is the thickness of scale layer,  $\lambda$  is the heat conductivity coefficient of scale layer, and  $\alpha$  is the heat transmission coefficient of reacting gas.

In the experiment process,  $T_g$  and  $\alpha$  were constants,  $T_w$ , especially at the water-cooled wall, was approximately treated as constant, too. Then the following formulas can be obtained

$$\frac{1}{\delta}(T_s - T_w) = c_1(T_g - T_s) \quad (2)$$

or

$$c_2(T_s - T_w) = \delta(T_g - T_s) \quad (3)$$

where both  $c_1$  and  $c_2$  are constants.

It can be obtained that  $T_s$  increases with the increase

of scale layer thickness. The thicker the scale is, the closer  $T_s$  to  $T_g$ ; the thinner the scale is, the closer  $T_s$  is to  $T_w$ . Obviously, if the scale layer is thin enough,  $T_s$  is low enough, neoformative particles are incompact and could not be fused or sintered. If they are cleared instantaneously, the radial growth of scale could be controlled. Otherwise, the ultrafine particles are easy to be coagulated and aggregated at high temperature and a particle-packed layer is formed on the reactor wall surface. Once this layer reaches a given thickness, the scale surface temperature is adequately high, the deposited particles will be sintered each other and the scale layer will be rapidly built-up and it is difficult to remove[10].

Besides, alteration of phase composition with thickness increase of scale layer should be calculated. Crystalline  $TiO_2$  particles produced industrially are in the crystal form of anatase or rutile. The formation of  $TiO_2$  crystallites in the oxidation reactor is shown as the following gas-phase reaction:



$TiO_2$  monomers generated by reaction (4) can form metastable anatase clusters by homogeneous nucleation. Then, the clusters grow by the heterogeneous condensation of  $TiO_2$  vapor and the coagulation-fusion of new particles[11]. Some of them become anatase particles, and others are transformed to rutile particles, which are thermochemically stable[12].

Without additive  $AlCl_3$  as a crystal conversion agent, phase composition of most neogenic  $TiO_2$  particles is anatase in the experiment. Conversions active energy from anatase to rutile is 460 kJ/mol. As temperature rises, crystal conversion rate will increase like the mass fraction of rutile will increase[13, 14]. Hence, after a lot of heat accumulated, phase composition of particle-sintered layer was characterized to be rutile phase.

### 3.3 Axial temperature distribution in reactor

Along the length of the tube, there was an isothermal region measured by a copper-constantan (K type) thermocouple. The isothermal curve of the reactor tube at 1 100 °C is described in Fig.6, and the range of isothermal region is determined about 600 mm.

After the experiment was finished, it could be observed there were scales growing on the reactor inside wall and rods surface, but the scale layer distribution was uneven. The most severely scaled region was at the site 200–300 mm away from  $TiCl_4$  entrance where temperature was just close to isothermal region. Then the scale became smooth step-by-step from front to rear reactor.

The SEM images shown in Fig.7 are scale layers

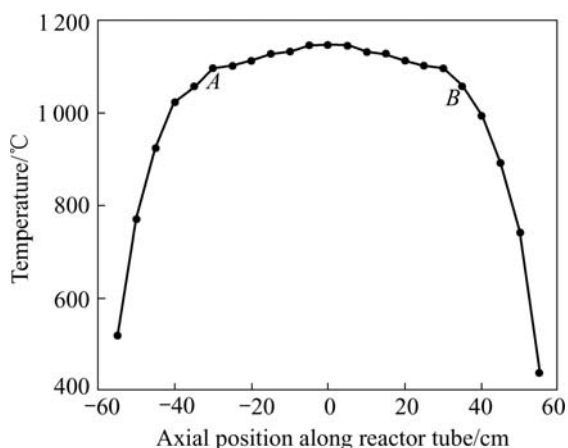


Fig.6 Temperature profile of reactor at 1100 °C

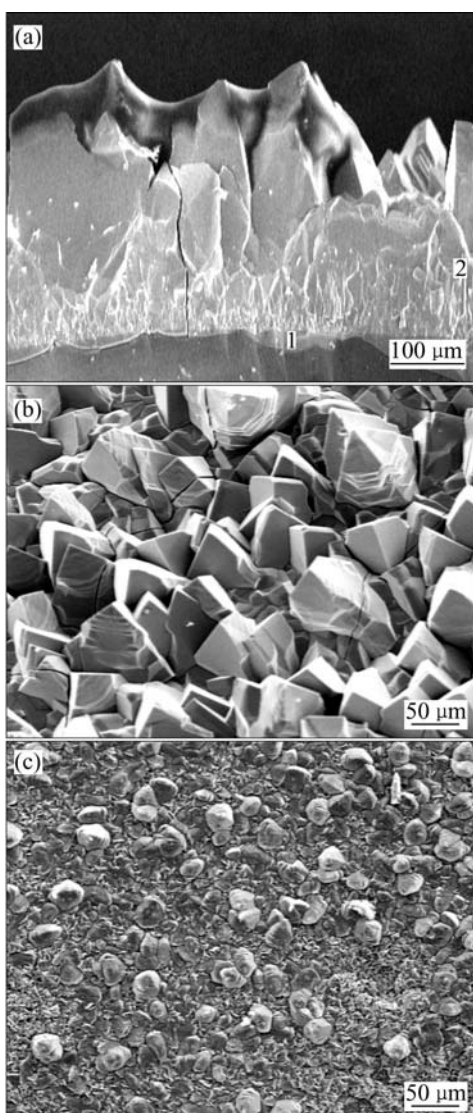


Fig.7 SEM images of scales: (a) Scale layer profile (1 Substrate; 2 Scale layer); (b) Scale stripped from front rod; (c) Scale stripped from rear rod

stripped from different sections of quartz rod. Fig.7(a) shows a cross sectional profile of scale layer from the severe scaled point which is remarked in Fig.6 as A.

Level 1 is quartz rod substrate; scale tightly appressed to level 1 is named level 2. It can be seen from Fig.7(a) that there is no obvious interface between the scale and quartz substrate. The positive face of this scale block is shown in Fig.7(b) and the scale stripped from the smooth scaled point is shown in Fig.7(c), which is remarked in Fig.6 as B. Compared with Fig.7(b), there are less agglomerations and shorter whisker columns in Fig.7(c). The XRD patterns shown in Fig.5(b) are scales on different sections of quartz rod (remarked in Fig.6 spot A and B). It is obvious that the scale from front rod was characterized to be rutile phase and scale from rear rod was partial anatase phase.

The reaction routes of TiO<sub>2</sub> scale formation can be described as Fig.8. According to the law of chemical gas phase deposition<sup>[15]</sup>, the dominating reactions are (a) and/or (a)→(b)→(f) under smooth reaction condition, while (c)→(d) and/or (c)→(e)→(f) under severe reaction condition[8, 16].

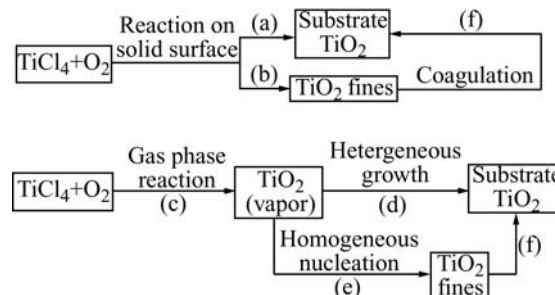


Fig.8 Reaction routes for formation of TiO<sub>2</sub> scale

Under our experimental conditions, general reaction was severe. Due to the existence of an about 600 mm isothermal region, temperature distribution in reactor was nonuniform. Temperature of both entrance and outlet was rather lower than that of intermediate section. Where temperature was high, the reaction was severe and fast. So, at the site 200–300 mm away from the entrance, the temperature was the highest, the scale layer was the thickest and the whisker column was the longest there. The reaction route in this zone should be (c)→(e)→(f). When the concentration of TiO<sub>2</sub> monomers and clusters were improved with the increase of temperature, the probability of homogeneous nucleation was enhanced in the same way. Scale surface shown in Fig.7(b) was just produced by this route. In contrast, the dominating reaction route should be (c)→(d) in the lower temperature region. TiO<sub>2</sub> monomers and clusters were deposited on the reactor wall and a thin continuous film was formed. Especially, because of heterogeneous growth of TiO<sub>2</sub> monomers, the film grew thick and compact, which can be seen in Fig.7(c). In the above two processes, the coagulation and aggregation of TiO<sub>2</sub> particles resulted in a hard scale being formed.

## 4 Conclusions

The gas-phase oxidation of  $\text{TiCl}_4$  in a high temperature tubular flow reactor can generate  $\text{TiO}_2$  scale deposition on the reactor wall. The state of reactor wall has little effect on scaling formation. With uneven temperature distribution along axis of reactor, the higher the reaction temperature is, the thicker the scale layer and the more compact the scale structure are. The scaling process can be deduced from the law of chemical gas phase deposition. At high temperature region, the dominated processes are gas phase reaction, homogeneous nucleation and fine particles/clusters coagulation. However, at the low temperature region, the dominated processes are gas phase reaction and heterogeneous growth.

## References

- [1] SUYAMA Y, KATO A. Effect of additives of the formation of  $\text{TiO}_2$  particles by vapor phase reaction[J]. *J Am Ceram Soc*, 1985, 68: 154–156.
- [2] AKHTAR M K, XIONG Y, PRATISINIS S E. Vapor synthesis of titania powder by tetrachloride oxidation[J]. *AIChE J*, 1991, 37: 1561–1570.
- [3] AKHTAR M K, PRATISINIS S E. Dopants in vapor-phase synthesis of titania[J]. *J Am Ceram Soc*, 1992, 75: 3408–3416.
- [4] SHI L, LI C, CHEN A. Morphology and structure of nanosized  $\text{TiO}_2$  particles synthesized by gas-phase reaction[J]. *Mater Chem Phys*, 2000, 66: 51–57.
- [5] AKHTAR M K, VEMURY S, PRATISINIS S E. Competition between  $\text{TiCl}_4$  hydrolysis and oxidation and its effect on product  $\text{TiO}_2$  powder[J]. *AIChE J*, 1994, 40: 1183–1192.
- [6] CHANG W, SKANDAN G, HAHN H. Chemical vapor condensation of nanostructured ceramic powders[J]. *Nanostructure Mater*, 1994, 4: 345–351.
- [7] CHANG W, SKANDAN G, DANFORTH S C. Chemical vapor processing and application for nanostructured ceramic powders and whiskers[J]. *Nanostructure Mater*, 1995, 6: 321–324.
- [8] MOROOKA S, OKUBO T, KUSAKABE K. Modification of submicron particles by chemical vapor deposition in fluidized bed[J]. *Powder Tech*, 1990, 63: 105–114.
- [9] SUPURR R A, MYERS H. Quantitative analysis of anatase-rutile mixture with a X-ray diffractometer[J]. *Anal Chem*, 1957, 29: 760–762.
- [10] JIANG H, LI C, LU Z, CONG D, ZHU Y. Scaling mechanism on the oxidation reactor wall in  $\text{TiO}_2$  synthesis with chloride process[J]. *J East China University of Science and Technology*, 2001, 27: 152–156.
- [11] XIONG Y, PRATISINIS S E. Gas phase production of particles in reactive turbulent flows[J]. *J Aerosol Sci*, 1991, 22: 637–642.
- [12] KOBATA A, KUASKABE K, MOROOKA S. Growth and transformation of  $\text{TiO}_2$  crystallites in aerosol reactor[J]. *AIChE J*, 1991, 37: 347–359.
- [13] COBLENZ W S, DYNYS J M, CANNON R M. Initial stage solid state sintering models: A critical analysis and assessment[J]. *Mater Sci Res*, 1980, 13: 141–157.
- [14] MACHENZIE K. The calcinations to titania: the effect of additive on the anatase-rutile transformation[J]. *Trans J Br Ceram Soc*, 1975, 74: 29–34.
- [15] MA S, XU K, JIE W. TiN coating on wall of holes and stitches by pulsed DC plasma enhanced CVD[J]. *Trans Nonferrous Met Soc China*, 2003, 13(4): 898–901.
- [16] ZHU Y, CHEN A, LI C. Mechanism of powder deposition on cool wall during the process of chemical synthesis of  $\text{TiO}_2$  in vapor phase[J]. *J East China University of Science and Technology*, 1999, 25: 382–385.

(Edited by LI Xiang-qun)